8-1-2009

Differential gene expression during compensatory sprouting of dendrites in the auditory system of the cricket Gryllus bimaculatus

H. W. Horch
Bowdoin College

S. S. McCarthy
Bowdoin College

S. L. Johansen
Bowdoin College

J. M. Harris
Bowdoin College

Insect Molecular Biology (2009) **18**(4), 483–496 doi: 10.1111/j.1365-2583.2009.00891.x

Differential gene expression during compensatory sprouting of dendrites in the auditory system of the cricket *Gryllus bimaculatus*

H. W. Horch, S. S. McCarthy, S. L. Johansen and J. M. Harris*

Bowdoin College, Department of Biology and Neuroscience, Brunswick, ME, USA

Abstract

Neurones that lose their presynaptic partners because of injury usually retract or die. However, when the auditory interneurones of the cricket *Gryllus bimaculatus* are denervated, dendrites respond by growing across the midline and forming novel synapses with the opposite auditory afferents. Suppression subtractive hybridization was used to detect transcriptional changes 3 days after denervation. This is a stage at which we demonstrate robust compensatory dendritic sprouting. Whereas 49 unique candidates were down-regulated, no sufficiently up-regulated candidates were identified at this time point. Several candidates identified in this study are known to influence the translation and degradation of proteins in other systems. The potential role of these factors in the compensatory sprouting of cricket auditory interneurones in response to denervation is discussed.

Keywords: suppression subtractive hybridization, denervation, invertebrate.

Introduction

Within the nervous system, the shape and position of any neurone's dendritic arbor will influence its pool of potential synaptic partners. Historically, dendritic morphogenesis was thought to be predominantly determined by intrinsic genetic factors, and indeed, partial dendritic development has been shown to proceed in isolated neuronal cultures (Bartlett & Banker, 1984). However, experiments over the last two decades have shown that dendrites respond to a range of intrinsic and extrinsic factors (reviewed in McAllister, 2000; Scott & Luo, 2001; Kim & Chiba, 2004; Cline & Haas, 2008), and, importantly, that dendrites can be guided by the same proteins that influence axonal growth (Polleux *et al*., 2000; Whitford *et al*., 2002; Furrer *et al*., 2003). Furthermore, injury in mature neural systems appears to alter the expression of developmental guidance cues (Miranda *et al*., 1999; De Winter *et al*., 2002; Niclou *et al*., 2006), implying that the function of these cues may be recapitulated after injury.

One of the extrinsic factors that influence the maturation of dendritic form is presynaptic input. The synaptotrophic hypothesis states that synaptic inputs influence the elaboration of dendritic arbors (Vaughn, 1989), and there is good evidence that synaptic input is required for the normal development of dendritic structure in the mammalian brain (reviewed in Cline & Haas, 2008). The hypothesis further states that growing processes are stabilized by synaptic contacts. Consistent with this, removing presynaptic terminals usually destabilizes dendritic arbors, and a number of different types of postsynaptic responses have been reported (reviewed in Sherrard & Bower, 1998). The variety of observed responses is likely to be dependent on many factors such as age, cell type, and how profound the denervation is. However, it is clear that removing the predominant presynaptic input from developing neurones usually leads to negative effects on the postsynaptic neurone, including profound dendritic retraction (Benes *et al*., 1977; Deitch & Rubel, 1984) or even cell death (Parks, 1979; Born & Rubel, 1985; Sherrard & Bower, 1998; Baldi *et al*., 2000).

There are important exceptions to the typically negative response of developing dendrites to the removal of presynaptic input, or denervation, and studying them can inform our understanding of the factors that influence dendritic development, maintenance and plasticity (Hoy *et al*., 1985; Lakes *et al*., 1990; Pyapali & Turner, 1994).

First published online 5 May 2009.

Correspondence: Hadley Wilson Horch, Bowdoin College, Department of Biology and Neuroscience, 6500 College Station, Brunswick, ME 04011, USA. Tel.: +1 207 798 4128; fax: +1 207 725 3405; e-mail: hhorch@bowdoin.edu

*Current address: Pathology Department, Beth Israel Deaconesses Medical Center, Center for Life Sciences, Boston, MA, USA

One of the more striking examples of a positive dendritic response to denervation is the compensatory growth of auditory interneurone dendrites after denervation in the cricket auditory system (Hoy *et al*., 1985; Schildberger *et al*., 1986). The auditory system of the cricket is crucial to its survival and reproduction. Crickets perform negative phonotaxis to the ultrasound pulses of predatory bats (> 20 kHz) and female crickets perform positive phonotaxis to the calls of male conspecifics (5 kHz). The cricket auditory system consists of foreleg tympanal membranes, which overlie the tympanal organ and whose auditory receptor neurones project via the tympanal nerve (nerve 5) into the first ganglion of the thorax, the prothoracic ganglion (reviewed in Ball *et al*., 1989). Auditory afferents convey acoustic information to several different types of interneurones (Fig. 1A), most of which exist in mirror image pairs.

One auditory interneuron, ascending neurone-2 (AN-2) is used here to exemplify the denervation-induced changes in all auditory neurones examined (Schildberger *et al*., 1986). Normally, a majority of AN-2 dendrites grow up to but not over the midline of the prothoracic ganglia (arrow, Fig. 1A). Its dendrites receive auditory information from ipsilateral auditory afferents (grey 'claw' in Fig. 1A), which is then processed and relayed to the brain via an ascending axon (arrowhead, Fig. 1A). Denervation of the auditory interneurones can be achieved through unilateral removal of the prothoracic leg, which removes the auditory organ, and results in the degeneration of the auditory afferents (Fig. 1B). Removal of the cricket ear in a first instar larval nymph induces denervated AN-2 dendrites to grow across the midline (arrow, Fig. 1B), a boundary they usually observe, and form functional synaptic connections with the auditory afferents from the opposite ear by adulthood (Hoy *et al*., 1985; Schildberger *et al*., 1986). This compensatory synapse formation is remarkably precise, reinstating interneurone-specific threshold and intensity responses (Schildberger *et al*., 1986). This phenomenon may also explain how monaural females can recognize and roughly localize singing males (Huber *et al*., 1984). As physiological recordings do not reliably detect auditory responses in the auditory interneurones of preadult nymphs, the rate of functional recovery can only be assessed in the adult. Acute denervation experiments in adults have indicated that deafferented auditory neurones also sprout new projections that are capable of forming new synaptic connections with the opposite afferents 4–6 days postdenervation (Brodfuehrer & Hoy, 1988).

Given the robust nature of the compensatory growth of dendrites in the cricket auditory system, we used suppression subtractive hybridization (SSH) to ask which genes are differentially expressed after denervation. In the hopes of identifying candidates that might facilitate this positive growth response and synapse formation, we chose to investigate gene expression changes 3 days postdenervation in late-instar nymphs. Given that functional recovery has been documented in the adult as early as 4 days after denervation (Brodfuehrer & Hoy, 1988), this 3-day time point was selected in order to correspond with the point at

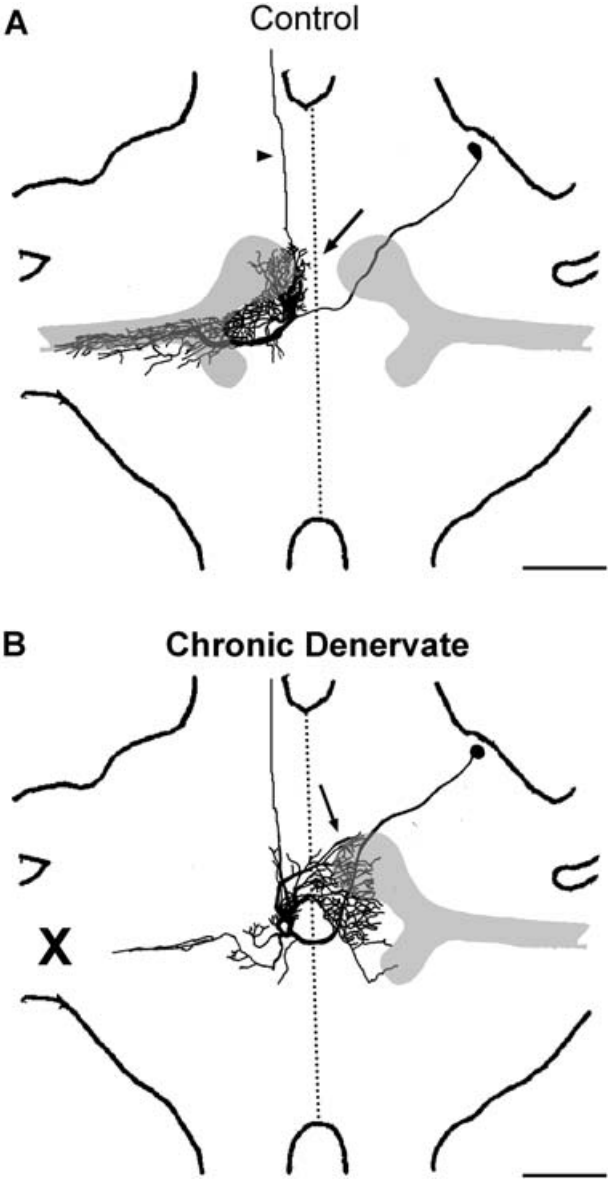

Figure 1. Chronic denervation results in profound reorganization of auditory interneurone dendrites in the cricket *Gryllus bimaculatus*. (A) Traced reproduction of a confocal image of a control ascending neurone-2 (AN-2) backfilled with biocytin in the adult cricket prothoracic ganglion. Bilateral auditory afferents are shown in light grey and arborize in a 'claw-shaped' end. The soma is contralateral to the main dendritic arbor and relevant auditory afferents, and a majority of the AN-2 dendrites respect the midline (arrow). The axon carries auditory information to the brain (arrowhead). (B) Auditory interneurones can be denervated by amputation of the leg, which leads to degeneration of the auditory afferents (X). Denervation throughout the nymphal instars of the animal results in a profound reorganization of AN-2 dendrites in the adult. A large proportion of the dendrites have crossed the midline and arborize in the contralateral auditory neuropil. Scale bars = approximately 100 μm.

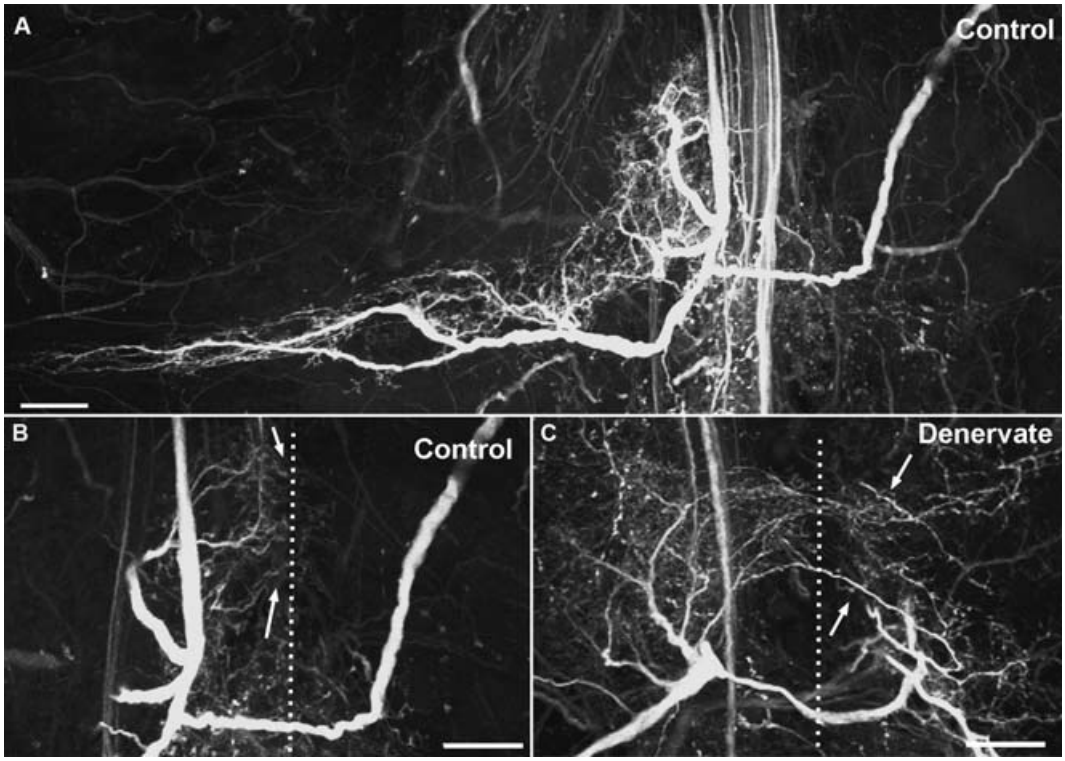

Figure 2. Dendritic reorganization is evident three days after denervation in antepenultimate instars. Confocal images of biocytin-filled ascending neurone-2 (AN-2). (A) Biocytin backfill of a control AN-2 (projection of 73 optical sections) reveals typical dendritic morphology. Midline is to the right of the image. (B) and (C) are images of the midline region of AN-2 and, for clarity, are presented as a projected subset of the sections that make up the whole volume of each cell. (B) Biocytin backfill of control AN-2 (40 optical sections) shows dendrites growing up to (arrows), but not over the midline (dotted line). (C) Biocytin backfill of AN-2 denervated on the left side (70 optical sections) shows obvious midline crossing of dendrites towards the right side (arrows). Scale bars = 20 μm.

which dendrites were actively growing across the midline and perhaps beginning to form synapses. Semiquantitative reverse-transcriptase-PCR (SQ-RT-PCR) was used to independently confirm the differential expression of candidates after denervation. The role that candidate genes may play in the compensatory growth of cricket auditory interneurones is discussed.

Results

In designing the subtractive hybridization experiment, we needed to choose the best developmental stage and time postdenervation to investigate transcriptional changes. Although the most robust anatomical changes are evident in adults that have been chronically denervated throughout the approximately 40 days of nymphal development (as shown in Fig. 1), we assumed that the relevant transcriptional changes involved in the compensatory sprouting would be rapid and possibly short-lived. Therefore, we wished to harvest tissue only a few days after denervation. Unfortunately, because we have been unable to explore the anatomical results of denervation in young nymphs, first or second instar nymphs were not appropriate for this experiment. As little is known about the development of auditory interneurones, such as when the ascending neurone axons project to the brain, it was unclear whether our inability to backfill young nymphs was a technical or developmental limitation. However, as we could easily detect a robust response to denervation of the auditory interneurones in older nymphs, we chose to use these animals for the subtractive hybridization experiment.

Compensatory dendritic growth in the cricket auditory system

In the past, published backfills were performed using Lucifer yellow or cobalt and then photographed or traced (Hoy *et al.*, 1985; Schildberger *et al.*, 1986). Backfills of AN-2 can also be successfully performed using biocytin and confocal microscopy (Fig. 2). Compensatory dendritic growth is anatomically evident by 3 days postdenervation in antepenultimate nymphal instars. Whereas the majority of AN-2 dendrites from control animals (n = 3 backfills) respected the midline at this developmental stage (Fig. 2A,B), a number of long dendritic branches from the deafferented AN-2 (n = 4 backfills) were seen growing across the midline 3 days after denervation (Fig. 2C). Although we did not quantify aspects of dendritic projections about the midline, there was little variability in the results, and the rapid

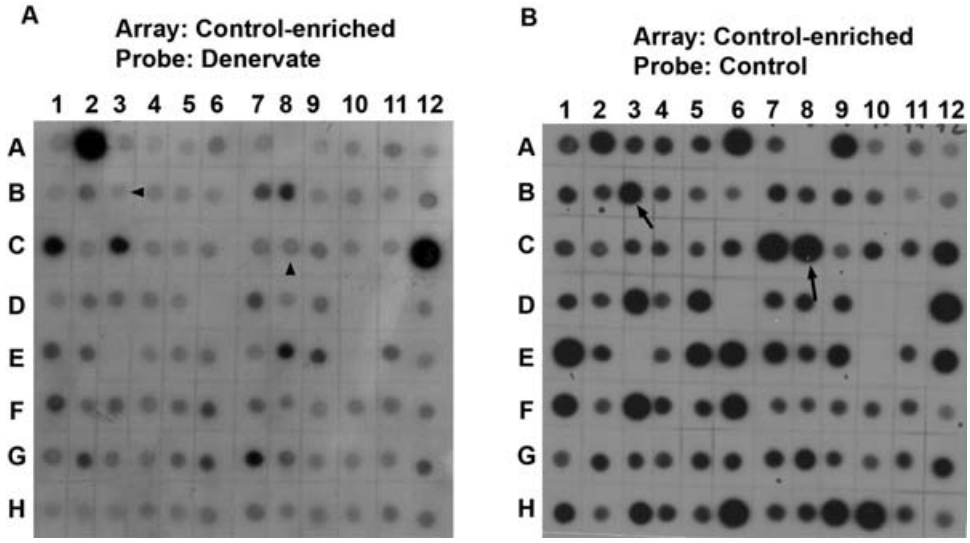

Figure 3. Example of the differential screening of the control-enriched library. Plasmid inserts from the control-enriched library were amplified and arrayed on duplicate nylon membranes (A and B). (A) The left membrane was hybridized with radiolabelled probes made from the denervate-enriched cDNA pool. (B) The right membrane was hybridized with radiolabelled probes made from the control-enriched cDNA pool. Arrows in (B) indicate two examples of clones for which the control-enriched probes hybridized more strongly than did the denervate-enriched probes (arrowheads in A) indicating down-regulated candidates.

morphological changes we saw here are consistent with previous work demonstrating that compensatory sprouting in adult animals restores auditory function within 4–6 days after denervation (Brodfuehrer & Hoy, 1988). Although compensatory dendritic growth is obvious in adult animals as well, it does not appear quite as robust as the reorganization seen in preadult animals. For this reason, we chose to use antepenultimate instars for SSH experiments because vigorous dendritic growth across the midline was obvious at this stage (Fig. 2C).

Differential gene expression during compensatory dendritic growth

SSH was used to identify differentially expressed genes throughout the prothoracic ganglia 3 days after denervation. We chose to examine the expression in whole ganglia, as opposed to halves or quadrants, because we made no *a priori* assumptions as to where the transcriptional changes would take place. Although transcriptional changes in the auditory interneurones themselves were likely, changes in the expression of genes at the midline might be equally important and would be lost if the ganglia were halved or quartered before proceeding. Therefore, the genes expressed in whole prothoracic ganglia of 3-day denervated antepenultimate instars were compared with those expressed in ganglia from control animals, which had received a tibial amputation (sparing the ear) 3 days previously. Both forward and reverse subtraction was performed in order to identify up- and down-regulated transcriptional changes after denervation. For both libraries, the white to blue colony ratio was 65:35, and 95% of the white colonies contained plasmids with inserts.

Differential screening was performed in order to identify differentially expressed candidates. To identify genes down-regulated after denervation, 288 control-enriched clones were selected and arrayed on nylon membranes in duplicate. A representative example (blot C1) is shown in Fig. 3. The left membrane was hybridized with probes made from the denervate-enriched library (Fig. 3A), and the right was hybridized with probes made from the control-enriched library (Fig. 3B). Clones that hybridized at least twofold more strongly with the control-enriched probes, such as B3 and C8 (arrows, Fig. 3B) than to the denervate-enriched probes (arrowheads, Fig. 3A) were defined as positive 'hits'. Differential screening of 288 clones from the control-enriched library yielded a total of 120 clones defined as positive hits. Conversely, to identify genes up-regulated after denervation, 288 denervate-enriched clones were similarly screened (Fig. 4). Surprisingly, none of the denervate-enriched clones showed a twofold enhancement of hybridization to the denervate probes (Fig. 4A) as compared to the control probes (Fig. 4B), meaning that none of the 288 clones screened was defined as up-regulated. Some of the denervate-enriched clones, such as A12, B12, D4, or H11 appeared to hybridize slightly more to the denervate-enriched probes than the control-enriched probes (Fig. 4). However, as they did not meet the twofold criteria, they were not defined here as up-regulated.

The 120 control-enriched clones identified through differential screening were sequenced, then translated and analysed using the National Center for Biotechnology Information (NCBI) website. A total of 49 unique candidates was identified as down-regulated 3 days after denervation (Tables 1 and 2). Candidates were named first by blot (ie

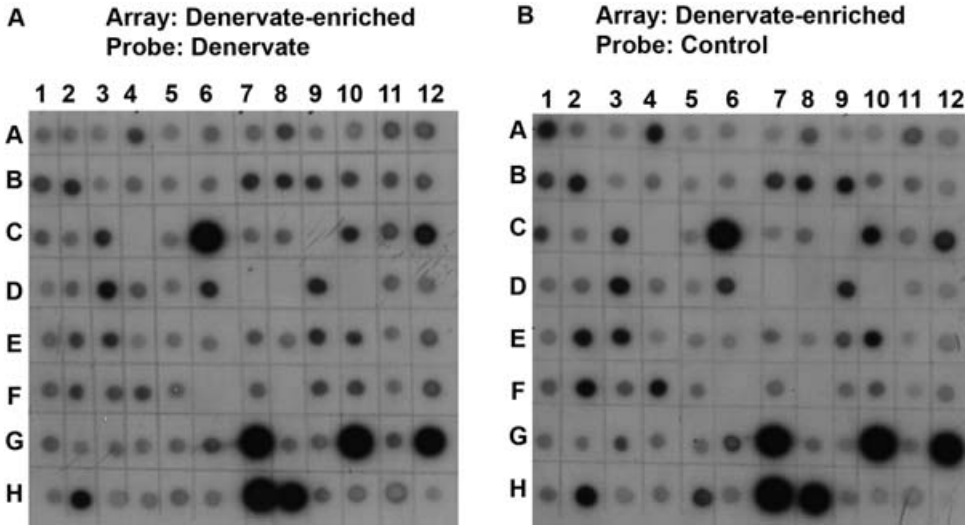

Figure 4. Example of the differential screening of the denervate-enriched library. Plasmid inserts from the denervate-enriched library were amplified and arrayed on duplicate nylon membranes (A and B). (A) The left membrane was hybridized with radiolabelled probes made from the denervate-enriched cDNA pool. (B) The right membrane was hybridized with radiolabelled probes made from the control-enriched cDNA pool. There were no examples of probes made from the denervate-enriched cDNA pool (A) hybridizing at least twofold more than did the control-enriched probes (B).

Table 1. Twenty-two candidates identified as down-regulated 3 days after denervation were homologous to genes in other species and can be broadly grouped

Category	Representative clone (seq. no.)	*Gb* accession no.	Size (bp)	Best match description	*E*-value	Best match accession no.	% Identity/ % similarity	Species of best match
Enzyme	**C2A4**	**GE653135**	**334**	**alcohol dehydrogenase**	**4.00*E*-24**	**NM_001101887.1**	**53/75**	***Bos taurus***
	C1B3 (14)	**GE653162**	**633**	**alpha-amylase**	**1.00*E*-33**	**AF527876.1**	**78/89**	***Anthonouus grandis***
	C1H8	GE653138	128	alpha-amylase	1.00*E*-08	AF208002	56/75	*Diabrotica virgifera virgifera*
	C2A12 (8)	GE653128	332	alpha-amylase	4.00*E*-33	AF467104.2	57/72	*Megaselia scalaris*
	C2A7 (2)	GE653152	418	alpha-amylase	3.00*E*-38	DQ355516	68/79	*Blattella germanica*
	C3C12 (2)	GE653137	246	alpha-amylase	7.00*E*-26	EF600049.1	71/76	*Helicoverpa armigera*
	C3F10 (9)	GE653155	549	alpha-amylase	7.00*E*-62	DQ355516.1	74/84	*Blattella germanica*
	C3C10	GE653136	247	beta-1,4-endoglucanase	7.00*E*-14	AJ511343.1	69/81	*Mastotermes darwinensis*
	C1F1 (6)	GE653141	175	*bimac.* EST: lysozyme	3.00*E*-52	AY226458	63/78	*Gryllus bimaculatus*
	C3F11	GE653156	543	cytochrome oxidase I (mit)	6.00*E*-75	GPU88332	91/93	*Gryllus pennsylvanicus*
	C2B8	GE653134	272	oxidoreductase	5.00*E*-05	XM_001844134.1	55/78	*Culex quinquefasciatus*
	C1A6 (10)	GE653118	461	salivary lysozyme	2.00*E*-35	AY226458.1	63/76	*Anopheles stephensi*
	C1A5 (2)	GE653117	442	trehalase	6.00*E*-4	AJ512337	47/67	*Caenorhabditis elegans*
	C2H7 (2)	GE653127	368	trehalase	3.00*E*-27	NM_001112671.1	47/67	*Apis mellifera*
	C3H9	GE653149	284	trehalase	3.00*E*-20	D11338	59/75	*Tenebrio molitor*
Protein degradation	**C2F2**	**GE653126**	**505**	**pushover**	**3.00*E*-46**	**AF096896**	**53/74**	***Drosophila melanogaster***
	C1H4	**GE653145**	**290**	**ubiquitin specific protease**	**2.00*E*-26**	**XM_001897165**	**76/88**	***Brugia malayi***
Protein synthesis	C3D1	GH160416	222	ribosomal protein S8	6.00*E*-23	EF638994.1	86/92	*Triatoma infestans*
	C1G9	GE653143	311	serine carboxypeptidase	9.00*E*-33	AY962406	65/78	*Sitodiplosis mosellana*
	C3C5	GE653131	335	translation initiation factor 3	9.00*E*-40	XM_001842255	71/89	*Culex quinquefasciatus*
Stress response	**C1A9**	**GE653119**	**284**	**Pr-5-like protein**	**2.00*E*-23**	**AY863030**	**77/82**	***Lysiphlebus testaceipes***
	C3F3 (4)	GE653160	413	regucalcin	3.00*E*-31	NM_205746	53/71	*Danio rerio*

Candidates are listed in groups, which are identified on the left. The clone number for each candidate identified is given (second column). In cases where the sequences of multiple clones overlapped, a representative clone number is listed and the number of matching clones is included in parentheses. Candidates in bold were used in the semiquantitative reverse-transcriptase-PCR experiment (Fig. 7). The *Gryllus bimaculatus* sequences we identified have been submitted to GenBank, and their accession numbers are listed in the '*Gb* accession no.' column. In order to identify each of these candidates, the full sequences were blasted using the 'tblastx' feature of the National Center for Biotechnology Information database against the nucleotide collection (nr/nt) database, and the best annotated Insecta match was identified when possible. Thus, for each candidate the 'description' of the best match, the *E*-value for the best match, the accession number of the best match, the predicted percent identity (identical amino acids) and predicted percent similarity (similar amino acids) to the best match, and the species of the best match are given. The only mitochondrial match was C3F11 (cytochrome oxidase) and this is indicated with a '(mit)'. Candidates whose *E*-values were greater than 0.001 were defined as 'NSH' (no significant hits) and included in Table 2.

C1) and then by row and column (ie B3), as in C1B3. An arbitrary cutoff of $E \leq 0.001$ (expectation value) was applied, which resulted in 27 candidates being defined as having no significant hits (NSH, Table 2). One of the candidates, C3F11, showed high homology to cytochrome oxidase, and was the only mitochondrial candidate identified through our screen. Some of the candidates were represented by multiple clones, for example, two of the unknown candidates,

Table 2. Twenty-seven candidates did not match any database entries and are defined here as 'no significant hits'

Representative clone (# seq)	*Gb* accession no.	Size (bp)
C1C6	GE653142	322
C1C12 (3)	GE653150	209
C1D1	GE653166	195
C1D12 (8)	GE653120	565
C1D9	GE653158	433
C1G3	GE653129	465
C1G5	**GE653132**	**441**
C1H1	GE653122	155
C2A8	GE653121	233
C2B6	GH160417	521
C2C2	GE653157	188
C2C5	GE653133	220
C2D1 (2)	GE653154	586
C2D5	**GE653123**	**372**
C2D9	GE653153	291
C2E3	GE653124	319
C2F6	GE653140	330
C3A9	GE653159	277
C3B2	GE653139	199
C3B6 (2)	GE653144	535
C3C4 (5)	GE653130	308
C3D6	GE653165	372
C3E8	**GE653163**	**340**
C3F1	GE653164	275
C3F6	GE653161	250
C3H1	GE653146	278
C3H7 (8)	GE653148	317

Those candidates whose *E*-values were greater than 0.001 were labelled as 'NSH' (no significant hits) and are listed here. The clone number for each candidate identified is given (first column). In cases where the sequences of multiple clones overlapped, a representative clone number was listed and the number of matching clones was included in parentheses. Candidates in bold were used in the semiquantitative reverse-transcriptase-PCR experiment (Fig.7). The *Gryllus bimaculatus* sequences we identified have been submitted to GenBank, and their accession numbers are listed in the '*Gb* accession no.' column. The size of each clone is given.

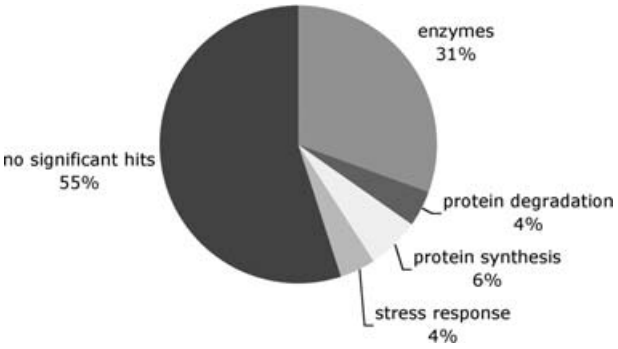

Figure 5. Distribution of the candidates according to their putative function. Functions were assigned, as detailed in Tables 1 and 2, based on the results of BLAST searches. 55% of candidates had no match in the database below $E = 0.001$ and were defined as no significant hits. 31% of the candidates encoded enzymes of a variety of functions. The remaining 14% of candidates fell into three categories: stress response, protein synthesis, and protein degradation.

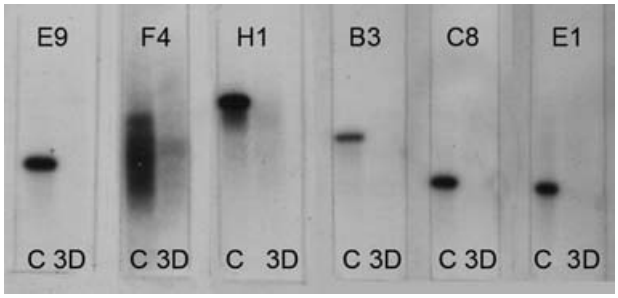

Figure 6. Virtual Northern blots were used to confirm the validity of the screen process. Of the control-enriched clones determined to be differentially expressed, six were randomly selected from the first differential screen and used to make ^{32}P-labelled probes. The original unsubtracted control (C) and denervate (3D) cDNAs were resolved on agarose gels and blotted onto nylon membranes. The binding of specific probes (labelled at the top of each blot) to the control but not denervate lanes is an indication of the accuracy of the original subtraction.

C1D12 and C3H7, appeared multiple times (Table 2). Clones matching alpha amylase, trehalase, salivary lysozyme, and regucalcin also appeared multiple times (Table 1). For the sake of comparison, those clones matching database entries were divided into categories (Table 1) including factors involved in general enzymatic function, stress response, protein degradation, and protein synthesis, and their relevant prevalence was calculated (Fig. 5).

Candidates known to be involved in the production of mature proteins included serine carboxypeptidase, translation initiation factor 3 subunit-8 (eIF-3-S8), and ribosomal protein S8. Two identified proteins, ubiquitin-specific protease and pushover, are involved in the process of protein degradation. Ubiquitin-specific proteases cleave ubiquitins from peptides, and E3 ubiquitin ligases, such as pushover, attach ubiquitin to proteins destined for degradation (Varshavsky, 1997). Candidates possibly involved in stress response included pathogenesis-related protein-5 (PR-5)-like protein and regucalcin (also known as senescence-marker protein 30), a calcium regulatory protein that may protect against oxidative damage in the brain (Son *et al*., 2006). A large number of enzymes was also identified. Two of the enzymes, alpha-amylase and trehalase, metabolize carbohydrates (Coimbra, 1966; Clifford, 1980), and are likely to regulate the supply of metabolic energy in the animal. Alcohol dehydrogenase has been shown to be one of the enzymes involved in the production of retinoic acid, a hormone well known to regulate gene expression and neuronal development in mammals (Duester, 1994). Hydrolytic enzymes and lysozymes are known to play a role in immunological defence in insects (Adamo, 2004; Schmid-Hempel, 2005).

In order to verify the accuracy of the screen in detecting differences in the SSH samples, six randomly selected control-enriched clones were used to make probes for virtual Northern blots. A portion of the original unsubtracted control and denervate cDNA was run on an agarose gel, blotted, and probed with these six probes (Fig. 6). For

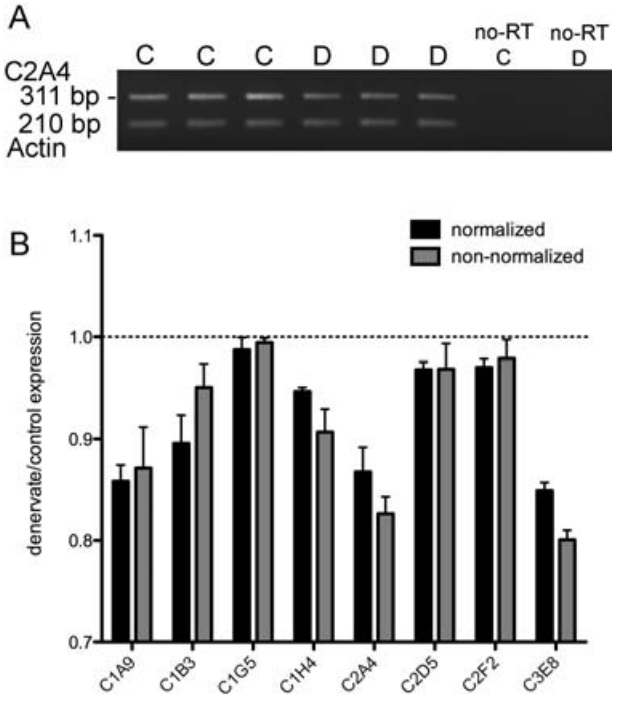

Figure 7. Semiquantitative reverse-transcriptase-PCR (SQ-RT-PCR) analysis exploring expression in an independent sample. (A) Example agarose gel of SQ-RT-PCR experiment. Pairs of primers for candidate C2A4 and actin were combined in multiplex reactions. Each reaction was set up in triplicate, and lanes are labelled with the template used: C, control; D, denervate; no-RT C, control RNA to which no RT was added; and no-RT D, denervate RNA to which no RT was added. (B) The expression level of the denervate lanes are expressed as a proportion of the normalized control expression and averaged for each triplicate. Black bars represent values normalized by the within-reaction actin, and grey bars represent non-normalized values. The error bars are the % error (SEM as a percent of the average). Chi-square analysis confirmed that these values are nonrandomly distributed below one ($P = 0.038$).

example, lanes B3 and C8 were hybridized with probes made from the clones highlighted by arrows in Fig. 3. In all six cases, strong bands were seen only in unsubtracted control cDNA and not in unsubtracted denervate cDNA, indicating that the identification of differentially expressed sequences from within the subtracted library was accurate.

Independent confirmation of down-regulated clones

Although the virtual Northern blots indicated that we could have confidence in the accuracy of the screen of the original tissue samples, it did not independently verify changes in expression of any of these candidates in additional tissue. To validate the differential expression in an independent tissue sample, the relative expression levels of eight of the identified candidates were independently characterized using SQ-RT-PCR. These eight candidates were chosen to represent a range of identified and novel candidates (Fig. 7). We purposefully chose several of the candidates that were represented by multiple clones. The gene-specific primers used in these experiments (Table 3) gave only a single band at the optimal cycle number. As described in the methods, multiplex reactions were run in triplicate (technical replicates) on a single control and denervate sample of pooled ganglia. The housekeeping gene, *β-actin*, was used for normalization. The normalized control bands were defined as 1, and normalized denervate values were expressed as a percent of control expression (black bars, Fig. 7B). Chi-square analysis indicated that the resulting values were not randomly distributed about '1', but instead confirmed that the denervate expression values were nonrandomly distributed below '1' ($P = 0.038$).

Although actin is routinely used as a housekeeping gene, its reliability has been questioned (Ruan & Lai, 2007). For example, actin has been shown to vary by gender, anatomical area, and type of experimental manipulation (Derks *et al.*, 2008). Importantly, the small variation we saw from reaction to reaction was bidirectional, indicating that it was unlikely that actin was differentially regulated after denervation. In addition, calculating non-normalized results for each candidate (grey bars, Fig. 7B) did not change our overall conclusion that the population of candidates showed a nonrandom distribution below '1'.

Discussion

The anatomical changes involved in the compensatory sprouting of dendrites in the cricket were first described

Table 3. Gene-specific primers used for the semiquantitative reverse-transcriptase-PCR experiment

	Left primer	Right primer
C1A9	AGAGTGCCTGTCTTGCCTTC	TTCCAGAAAAAGAGGTTGCAG
C1B3	GGAGCTCTTCACACCCTCAG	TACCCGGCTGTGTCCTACTC
C1G5	TGCCCAAAATTATACTTAACAAAGA	TGTGTGTTATTAGACGTGTTCGTG
C1H4	TACAGCCCCGCTGCTTTTAC	GGGACGGTCTAGCTCTAGTGG
C2A4	AGGTACGAGCGCCCTAGATG	GGCAAATTTTGTAGCTGCTTG
C2D5	ATCTTCTCTTTGGCGCATGT	CCATTGGTGATATTTCTTGTGC
C2F2	CTGCGCTTTGCCCAGGAGAA	CGAGGCCCTGATCTTGTCGTGTT
C3E8	TGCTCACTCCAGTTTGGTTTC	GCAGGTACCCATTTTGTTGAC
β-Actin	CCTGGCATTGCTGATAGGAT	CCTGCTTGGAGATCCACATT

Pairs of gene-specific primers for each of eight candidates tested amplified single bands at the optimal cycle number. Primers against *Gryllus bimaculatus* β-actin were used in each reaction for normalization.

over 20 years ago (Hoy *et al.*, 1985) and have been explored in a number of additional studies since that time (Pallas & Hoy, 1986; Schildberger *et al.*, 1986; Brodfuehrer & Hoy, 1988; Schmitz, 1989). The experiments presented here document profound anatomical changes by 3 days after denervation in antepenultimate instar nymphs and represent the first reported attempt to understand the molecular basis of this compensatory sprouting phenomenon in the cricket. Our subtractive hybridization results indicate that although down-regulated candidates were readily identified, the up-regulation of gene transcription may occur rarely if at all at this time point and possibly only in the small number of sprouting neurones.

Rapidity of dendritic changes after denervation

Morphological changes in the denervated AN-2 were evident 3 days after denervation. At this time point, many dendrites had grown across the midline, whereas control AN-2 dendrites typically respected the midline. The earliest reported morphological changes previously observed in the cricket are at 6 days postdenervation (Brodfuehrer & Hoy, 1988; Schmitz, 1989), although functional recovery has been reported as early as 4 days after denervation in the adult (Brodfuehrer & Hoy, 1988). It is unclear whether the discrepancy between our results and the timing of the previously published morphological changes in adult crickets is simply because of differences in developmental stages or sensitivity of more modern techniques. We suspect that the sensitivity of confocal microscopy, combined with the enhanced fluorescence and reduced photobleaching of newer fluorophores, reveal a much more detailed anatomical picture.

Exploration of other denervation paradigms reveals a variety of morphological and molecular changes that occur over a range of time courses. For example, the rate of denervation-induced dendritic growth in the locust auditory system appears similar to the cricket, with sprouting obvious within 5 days of denervation (Lakes *et al.*, 1990). In the chick auditory brainstem, denervation induces dendritic loss that is anatomically evident within an hour of denervation (Deitch & Rubel, 1984) and more pronounced within 7 h (Sorensen & Rubel, 2006). Microglial migration to the site of injury is evident in leeches within 24 h (Morgese *et al.*, 1983). Likewise, molecular changes in both invertebrates and vertebrates, such as alterations in the expression of tubulin, microtubule-associated proteins, and proteoglycans are often evident within 24 h of denervation (Kwak & Matus, 1988; Mostafapour *et al.*, 2002; Wang *et al.*, 2005; Schafer *et al.*, 2008; Wang & Rubel, 2008). Interestingly, time course experiments indicate that these mRNA and protein expression patterns usually persist for many days or even several weeks postdenervation (Kwak & Matus, 1988; Luthi, 1994; Schafer *et al.*, 2008; Wang & Rubel, 2008).

Given these results, we chose to examine transcriptional changes in preadult crickets 3 days after denervation. The 3-day time point seemed a best compromise that would allow us to identify early and maintained transcriptional changes induced by the denervation. In addition, we hoped to catch transcriptional changes responsible for the initial stages of synapse formation that would be likely occurring in anticipation of the functional recovery evident in adults by 4 days postdenervation.

Deciding in which developmental stage to perform these studies was also a challenge. Crickets are considered to be paurometabolous insects, as they go through a gradual, simple metamorphosis (Borror *et al.*, 1976). As such, the larval nymphs are typically very similar to adults, except adults have wings and are sexually mature, and nymphs go through a series of moults in order to increase body size. Although denervation-induced dendritic sprouting does occur in the adult auditory system, the morphological changes are less robust than in the late instar nymphs. Thus, we chose the time point with the most robust response in the hopes of identifying the most influential candidates. It is entirely possible that the transcriptional changes responsible for compensatory growth during development (nymphs) is distinct from that in adults. However, given the similarities in the central nervous systems of adults and nymphs, we have assumed that the changes that we identified in the nymphs will be generally applicable to the adult.

Transcriptional changes after denervation

We performed a SSH experiment to identify transcriptional changes 3 days after denervation. We used both a forward and a backward subtraction strategy in order to identify both up- and down-regulated genes. Whereas 120 clones were identified as down-regulated by at least twofold within 3 days after denervation, screening 288 clones in the opposite direction did not detect any candidates that were up-regulated by at least twofold. Although the absence of any sufficiently up-regulated candidates was unexpected, the down-regulation was, in fact, consistent with another denervation study that detected extremely rapid reductions in protein synthesis within 30 min of denervation in the chick auditory system (Steward & Rubel, 1985).

Alhough the cricket auditory interneurones respond to denervation by growing, perhaps the remaining denervated and axotomized neurones in the ganglion respond to denervation in a more typical or 'negative' fashion. As these non-auditory neurones represent the vast majority of cells in the ganglion, they may be responsible for some portion of the down-regulated candidates detected. In fact, the concept that the auditory interneurones are responding differently from most other denervated neurones is consistent with past work in the cricket that examined the effects of cercal ablation on the giant interneurones in the terminal ganglia. Unlike the auditory interneurones, giant

interneurones in the cricket do not respond to denervation by concerted sprouting across the midline, but instead typically show reduced dendritic length after denervation (Murphey *et al.*, 1975).

If selective up-regulation of transcription occurred only in the small number of auditory interneurones in the prothoracic ganglia, up-regulated candidate mRNAs would be likely to be of low abundance in the pooled mRNA from the entire ganglion. It is important to note that several clones showed hybridization patterns that were consistent with up-regulation, although at a subthreshold level. A different experimental design strategy, such as halving or quartering the ganglia before processing, might enhance the ability to detect small changes in a small number of neurones. However, this strategy would effectively eliminate the detection of any relevant changes that might be occurring at the midline or in an area remote to the auditory cell bodies. We chose to make no assumptions about the location of the transcriptional changes when designing this experiment and instead used whole ganglia for the experiment. However, re-evaluating our screen using a lower threshold might result in the identification of rare transcripts that are up-regulated. This strategy would also be likely to increase the number of false positives identified.

SSH is, in fact, an ideal technique to employ when trying to detect low abundance transcripts because of the normalization step, which equalizes the abundance of cDNAs within the target population (Diatchenko *et al.*, 1996). However, it might be necessary to screen at least 5000–10 000 clones isolated from the SSH cDNA libraries in order to detect a reasonable proportion of the low abundance transcripts (Cao *et al.*, 2001). Therefore, our initial screen of 288 clones may not have been sufficient to identify changes in rare transcripts. Alternatively, perhaps 3 days postdenervation was not the optimal time at which to detect transcriptional up-regulation.

Many of the candidates identified through this experiment matched nothing in the NCBI database (Table 2). Although it is exciting to contemplate the identification of novel factors that may be involved in this compensatory sprouting phenomenon, there are several reasons why known proteins could have appeared as 'no significant hits' in this study. First, the sequenced portion of the gene may have been in part of the gene that is not well conserved amongst species. Obviously more sequence information could be gathered from the cricket for each of these clones, which could help identify these candidates. In addition, the sequences may have represented noncoding RNAs whose regulatory function has not yet been identified (Genikhovich *et al.*, 2006). Or, finally, they may have represented novel genes with no known homologues. Given that we are working in an organism with little published sequence information and that crickets are separated by millions of years of evolution from other species for which genome sequences are available (Willmann, 2004; Buschbeck & Friedrich, 2008), more 5′ and 3′ sequence information will help clarify if these are truly novel genes or not.

A large number of enzymes was identified through this screen. We were most intrigued by a potential role for alcohol dehydrogenase in postinjury sprouting, because this enzyme is part of the multistep conversion of retinol into retinoic acid. Retinoic acid is well known to influence neuronal development and regeneration in mammals (Maden, 2001; Rawson & LaMantia, 2006), although its role in invertebrate nervous systems has been less clear. However, recent evidence indicates that retinoic acid induces neurite outgrowth and growth cone turning in invertebrate neurones (Dmetrichuk *et al.*, 2006). It is difficult to theorize how a down-regulation in alcohol dehydrogenase, which could presumably change the amount of retinoic acid available, would create an environment more permissible to dendritic growth. However, as retinoic acid is a transcription factor, one could imagine various scenarios in which decreases in retinoic acid levels reduce the transcription of growth inhibiting factors.

Many of the enzymes identified, such as alpha-amylase, trehalase, and lysozyme, may be involved in immune defence, stress response, and energy metabolism. Although it makes some sense that these enzymes might be modulated after injury, we would not have predicted that these enzymes would be down-regulated. Many of these enzymes are known to be components of haemolymph (Jahagirdar *et al.*, 1984; Adamo, 2004; Schmid-Hempel, 2005), although not necessarily neuronal tissue, so it is not clear why they were identified through this neuronal screen. The prothoracic ganglion is, of course, surrounded by haemolymph, and one possibility is that some of these enzyme candidates represent contaminants that were somehow processed along with the ganglia. This also implies that we consistently dissected denervated ganglia with less contamination than control ganglia in two separate experiments (SSH and SQ-RT-PCR), both of which consisted of pools of individual ganglia. As we can think of no systematic reason why contaminants would be biased towards control tissue, we have assumed that the down-regulation of these enzymes within neuronal tissue is a result of denervation. However, given the lack of known neuronal functions for many of these enzymes, it is difficult to speculate on their potential roles.

A selection of eight candidates used for SQ-RT-PCR independently confirmed the general validity of our SSH results (Fig. 7). Because this SQ-RT-PCR experiment consisted of a single sample of pooled ganglia for each condition it was not appropriate to confirm the quantitative extent of down-regulation for any individual candidate. Instead, examining the relative expression levels of the group as a whole indicated that our candidates were nonrandomly distributed below '1.' We assume that repeated independent confirmation of the differential expression of

all our candidates would both verify down-regulated candidates and identify several false positives. The false positive rate of SSH is generally accepted to be approximately 5 to 10% (cf. Cao *et al*., 2001; Jones *et al*., 2006). However, in practice, published results indicate a low rate of near 10% and a higher rate of 50 or even 60% (Qin *et al*., 2003; Jones *et al*., 2006; Pinter *et al*., 2006). The rigour of the verification process influences the number of false positives, and some of the variability in these false-positive rates across studies is likely to be the result of choice of technique used to independently confirm differential regulation. It would appear that it would be most informative to utilize a functional test in order to independently confirm the involvement of an identified candidate. Thus, in our future characterization of the candidates identified in Tables 1 and 2, we will supplement *in situ* hybridization and quantitative-PCR experiments with more functionally relevant tests, such as examining the effects of RNA interference on the compensatory growth of dendrites.

Protein translation and degradation in compensatory dendritic growth

Several of the candidates identified in our SSH experiment could act to influence protein levels in a transcription-independent manner. These results hint that denervation may induce changes at the level of protein translation and degradation in addition to those seen at the transcriptional level. Exciting work over the last few years has elucidated an important role for the proteasome system in synapse formation and synaptic plasticity (reviewed in Hegde & DiAntonio, 2002; DiAntonio & Hicke, 2004; Bingol & Schuman, 2005; Sutton & Schuman, 2005). The proteasome system has also been shown to influence the structure of developing neurones (Zhao *et al*., 2003). Although we had originally predicted that SSH would identify differentially regulated developmental guidance factors after denervation, transcriptional alterations in protein synthesis machinery or the ubiquitin proteasome system could specifically influence the levels of these types of proteins at the translational or post-translational level instead.

Our SSH identified two candidates, pushover and ubiquitin-specific protease 14, that are involved in the process of protein degradation via the ubiquitin proteasome system. This system involves a series of enzymes that attach a small, highly conserved peptide called ubiquitin to the N-terminus of proteins (Varshavsky, 1997). Ubiquitinated proteins are then recognized by specific proteasomes and digested. Pushover is a large, highly conserved ubiquitin ligase with a calmodulin binding domain, suggesting that pushover function may be calcium sensitive (Xu *et al*., 1998). Interestingly, several E3 ligases have been shown to regulate the expression of molecules involved in midline patterning in developing neuronal systems, including the slit receptor, roundabout, and components of the netrin signalling pathway (Campbell & Holt, 2001; Myat *et al*., 2002; Ing *et al*., 2007). In addition, examination of differential gene expression in the chick found that an E3 ubiquitin ligase, UBE3B, was strongly up-regulated after noise trauma (Lomax *et al*., 2000). In light of our results, the UBE3B work suggests that regulation of UPS function via E3 ubiquitin ligase transcriptional changes may be an important regulator of injury response in auditory systems.

Translational control of proteins can be rapid and profoundly influential as well. For example, rapid and local protein synthesis is necessary for the proper directional growth of developing axons. Guidance factors expressed during development, such as netrins and semaphorins, have been shown to activate translation initiation factors, which result in a rapid increase in local protein synthesis levels that then influences axonal growth (Campbell & Holt, 2001). Our SSH screen identified several proteins that could influence protein translation, including a translation initiation factor, that could potentially alter the way growing dendrites respond to existing guidance factors. In fact, there is evidence that injured pheochromocytoma cell (PC12) neuronal processes can regenerate rapidly in a transcription-independent manner (Twiss *et al*., 2000). These results underscore the fact that protein synthesis levels may be changing even though no alteration in transcription is detectable.

The SSH experiment presented here was a first step in understanding the transcriptional changes in individual genes or groups of genes that might influence the unusually robust compensatory sprouting seen in the cricket auditory system. Some of the transcriptional changes identified through this experiment indicate that more profound and specific changes may be occurring at the protein level. If the compensatory growth in this system were driven by post-translational protein regulation or modification, a proteomics screen would be a more effective way of identifying specific changes. We are in the process of performing a two-dimensional differential gel electrophoresis experiment that is better suited to identify differentially regulated or modified proteins. It is our hope that what we learn about this unusual and robust injury response in the cricket will expand our understanding of the control of dendritic growth and plasticity, and that this information may be applicable to the growth of dendrites in other neuronal systems.

Experimental procedures

Animals

A colony of Mediterranean field crickets, *Gryllus bimaculatus* (originally supplied by Dr Ron Hoy, Cornell University), was maintained on a 12:12 h light/dark cycle at 28 °C and 40–60% relative humidity. Crickets were fed commercial cat chow and drinking water *ad libitum*. Moist soil was offered for egg laying. Only crickets from this breeding colony were used for the described experiments.

Denervation and tissue collection

All crickets used in this study were treated identically throughout the experiment, with the exception of the type of surgery. Surgeries and tissue collections were performed side by side. Tissue was collected from crickets in the antepenultimate instar stage, which is the stage at which wing buds are first evident. Unilateral denervation of the central auditory neurones was accomplished by amputating the right prothoracic leg (foreleg) at or above the tibial femoral joint. Control crickets used for SSH were amputated at the right tarsal–tibial joint, leaving the developing auditory organ intact. All crickets used in this study were cooled to 4 °C prior to amputation and tissue collection. After surgeries were performed, crickets were grouped by condition (control or denervate) and housed for 3 days in small, shoebox-sized containers with adequate food, water, and hiding places. Three days postamputation, the prothoracic ganglia were dissected in RNase-free phosphate-buffered saline, frozen immediately in liquid nitrogen, and stored at –80 °C until processing. Control and denervated samples were amputated and dissected in parallel.

For backfill experiments, two types of denervations were performed. In the first, chronically amputated crickets were used to generate the schematic in Fig. 1. These crickets had legs removed initially during the first nymphal instar. These crickets were checked every few days and any regenerating blastema were removed. Once these animals matured into adults, AN-2 was backfilled (see below). The second type of backfill experiment was used to demonstrate the anatomical changes 3 days after denervation in antepenultimate instar nymphs (Fig. 2).

Biocytin backfills of AN-2 and microscopy

Anaesthetized crickets were immobilized by pinning and their thoracic cavity was opened. Approximately half to three-quarters of the axons in the appropriate neck connective were removed, leaving intact the medial–ventral portion containing the axon for AN-2. AN-2 was backfilled in the animal by retrograde uptake of 4% biocytin (Sigma, St Louis, MO, USA) dissolved in 50 mM $NaHCO_3$. Animals were maintained at 4 °C for 18–22 h. Ganglia were dissected and fixed in 4% paraformaldehyde (Electron Microscopy Sciences Hatfield, PA, USA), then treated with 0.5% triton and a 1:400 dilution of Alexafluor 488 streptavidin (Invitrogen, Carlsbad, CA, USA). Tissue was rinsed, dehydrated, and mounted in methyl salicylate. Images were collected using a Zeiss LSM 510 META and a 40X Plan Neofluor objective (1.3 NA, Zeiss, Thornwood, NY, USA). All images shown are projections of multiple optical sections, and the number of sections for each presented image is included in the figure legends. The midline was determined using three criteria, low power images were first used to roughly find the midline as defined by the point between the anterior and posterior intraganglionic connectives. Then, this general location was influenced by the characteristic point between the major L-shaped dendrite and the connective leading to the soma. Finally, viewing images at high gain made the autofluorescent cells of the midline evident, and the midline location was confirmed.

Confocal images were also used to create the schematic in Fig. 1. Briefly, one example of a control AN-2 and one example of a chronically denervated AN-2 were created from projections of multiple optical sections (151 and 141 optical sections, respectively), printed, and placed on a light box. Individual processes were then traced and a rough schematic outline of the ganglia was placed appropriately around each traced neurone. A backfill of nerve 5 was imaged with the confocal microscope and, as above, used to trace the extent of the auditory neuropil. Although the individual (H. W. H.) doing the tracing was not informed of the identify of each cell, the anatomical differences are such that the tracing could not realistically be performed blindly.

Suppression subtractive hybridization

Total RNA was purified, in parallel, from 10 control prothoracic ganglia (right tibia removed 3 days prior) and 11 denervated prothoracic ganglia (unilaterally amputated above tibial/femoral joint 3 days prior) using RNApure Reagent (GenHunter, Nashville, TN, USA) according to the manufacturer's protocol, and the subtractive hybridization was performed (Clontech, Mountain View, CA, USA). Briefly, amplified double-stranded cDNA was prepared for each condition from 300 ng total RNA as described in the SMART PCR cDNA Synthesis Kit (Clontech). First strand cDNA was diluted fivefold, and 1 μl of the dilution was used for PCR amplification (18 cycles). SMART-amplified cDNA was digested by RsaI endonuclease. SSH was performed in both directions (forward subtraction: 3-day denervate ganglia minus control ganglia, which will be referred to as denervate-enriched; and reverse subtraction: control ganglia minus 3-day denervate ganglia, which will be referred to as control-enriched). For each direction, two tester populations were created by ligating different suppression adaptors (Adaptor 1 or 2R). Each tester population was hybridized with 30-fold excess driver cDNA, and the two tester populations were hybridized together. Subtracted cDNA was amplified by primary PCR (25 cycles) and secondary (nested) PCR (10 cycles). The subtracted cDNA samples obtained by secondary PCR (control-enriched cDNA and 3-day denervate-enriched cDNA) were used for library construction. Forty ng of purified cDNA was cloned into the pAtlas vector and transformed into *Escherichia coli*.

Differential screening of subtracted libraries

Two-hundred and eighty-eight randomly picked white colonies from the control-enriched library and 288 randomly picked white colonies from the 3-day denervate-enriched library were used for differential screening. *E. coli* cultures were grown in 96-well format in 100 μl Luria broth with ampicillin (75 μg/ml) for 6 h at 37 °C. Plasmid inserts were amplified with F1S and R1S primers (5′-AGTACGCTCAAGACGACAGAA-3′ and 5′-AAAGCAGTGGTAACAACGCAG-3′, respectively), and 100 ng of PCR-amplified insert was arrayed onto duplicate nylon membranes and hybridized with ^{32}P-labelled subtracted control and subtracted 3-day denervate cDNA probes. Blots were imaged with a phosphoimager, and clones were considered positive if there was at least a twofold enhancement of probe binding as compared to its relevant duplicate.

Sequence analysis of candidates

Plasmids from 120 differentially expressed clones were purified and the inserts were sequenced using M13dir or M13rev plasmid primers. Sequence results were analysed using the BLAST web service at NCBI using the tblastx feature (http://blast.ncbi.nlm.nih.gov/Blast.cgi accessed November 2008). A threshold *E* value of 0.001 was used to determine the identity. Those candidates with larger *E* values were labelled as 'no significant hits' and listed separately (Table 2). When possible, a candidate's identity was defined as that hit with the lowest *E*-value, from the class Insecta, and that was annotated (Table 1).

Virtual Northern blots

A portion of the original, unsubtracted SMART-control and denervate cDNAs (used above for SSH) were resolved on agarose gels and transferred to Hybond-N membranes (GE Healthcare Biosciences Corp, Piscataway, NJ, USA). Membranes were hybridized with ^{32}P-labelled probes prepared from six control-enriched clones randomly selected from the first blot (C1E9, C1F4, C1H1, C1B3, C1C8, C1E1).

Semiquantitative RT-PCR

Tissue was dissected and pooled from an independent group of 33 control (tibia removed) and 32, 3-day denervate prothoracic ganglia (leg below tibial/femoral joint removed). Crickets for this experiment were handled in an identical manner as for the SSH experiments. RNA was purified using RNApure Reagent (GenHunter), DNaseI-treated with the MessageClean Kit (GenHunter), and quantified by an ND-1000 Nanodrop Spectrophotometer (Thermo Fisher Scientific, Wilmington, DE, USA). All samples were processed in parallel. Single-stranded cDNA was made from 3 μg total RNA using the Superscript III First-Strand Synthesis System for RT-PCR (Invitrogen). To check for genomic contamination, a 'no-RT' control was included for each sample. The first-strand synthesis reaction was diluted in order to allow reproducible and accurate aliquots (5 μl) to be removed for subsequent PCR reactions (Pernas-Alonso *et al*., 1999). Gene-specific primers (Table 3) for eight candidates as well as for *G. bimaculatus* β-actin (accession no. DQ630919) were designed using Primer 3 (Rozen & Skaletsky, 2000). Pilot experiments indicated that these were good primer pairs to use because single well-defined bands were amplified. For each primer pair, a cycle series was run on control cDNA in order to determine the optimal cycle number, defined as producing a product strong enough to detect on an agarose gel, but still in the preplateau, exponential range. Multiplex PCR reactions, using candidate-specific primers and β-actin-specific primers, were run in triplicate at the optimal cycle number on four different cDNA templates: (1) control; (2) denervates; (3) control 'no-RT'; and (4) denervate 'no-RT'. Amplified products were run on a 2% agarose gel with ethidium bromide and digitally photographed using a Bio Doc-It Imaging System transilluminator (Ultra-Violet Products, Upland, CA, USA). Digital images were saved for quantification.

Quantification of SQ-RT-PCR

Band intensity was measured using LabWorks software (Ultra-Violet Products). Background-subtracted intensity values were obtained for each band, and either used as they were, or were then normalized based on the measured β-actin band background-subtracted intensities for each lane. The normalized control values were defined as one, and the denervate values were expressed as a proportion of control for each primer set. The non-normalized data are included and are presented in the same manner. Percent error was calculated for each triplicate by dividing the SEM by the average. Standard error propagation was applied. A one-sided Fisher's exact test was used to assess significance.

Acknowledgements

This publication was made possible by NIH Grant Number P20 RR-016463 from the INBRE Program of the National Center for Research Resources, NIH Grant number 1 R15 DC006889-01 from NIDCD, and by an Alfred P. Sloan Research Fellowship. The authors would like to thank Dr J. Morgan, Dr M. Palopoli, Dr P. Dickinson, Dr A. McBride, and Dr B. Kohorn for thoughtful comments and advice.

References

Adamo, S. (2004) Estimating disease resistance in insects: phenoloxidase and lysozyme-like activity and disease resistance in the cricket *Gryllus texensis*. *J Insect Physiol* **50**: 209–216.

Baldi, A., Calia, E., Ciampini, A., Riccio, M., Vetuschi, A., Persico, A. *et al*. (2000) Deafferentation-induced apoptosis of neurons in thalamic somatosensory nuclei of the newborn rat: critical period and rescue from cell death by peripherally applied neurotrophins. *Eur J Neurosci* **12**: 2281–2290.

Ball, E.E., Oldfield, B.P. and Rudolph, K.M. (1989) Auditory organ structure, development, and function. In *Cricket Behavior and Neurobiology* (Huber, F., Moore, T.E., Loher, W., Huber, F., Moore, T.E. and Loher, W.S., eds.), pp. 391–422. Comstock Publishing Associates, Ithaca, NY, and London.

Bartlett, W. and Banker, G. (1984) An electron microscopic study of the development of axons and dendrites by hippocampal neurons in culture I. Cells which develop without intercellular contacts. *J Neurosci* **4**: 1944–1953.

Benes, F.M., Parks, T.N. and Rubel, E.W. (1977) Rapid dendritic atrophy following deafferentation: an electron microscopy morphometric analysis. *Brain Res* **122**: 1–13.

Bingol, B. and Schuman, E. (2005) Synaptic protein degradation by the ubiquitin proteasome system. *Curr Opin Neurobiol* **15**: 536–541.

Born, D. and Rubel, E. (1985) Afferent influences on brain stem auditory nuclei of the chicken: neuron number and size following cochlea removal. *J Comp Neurol* **231**: 435–445.

Borror, D., DeLong, D. and Triplehorn, C. (1976) The development and metamorphosis of insects. In *An introduction to the Study of Insects* (Borror, D., DeLong, D. and Triplehorn, C., eds.), pp. 72–84. Holt, Rinehard, and Winston, New York, NY.

Brodfuehrer, P.D. and Hoy, R.R. (1988) Effect of auditory deafferentation on the synaptic connectivity of a pair of identified interneurons in adult field crickets. *J Neurobiol* **19**: 17–38.

Buschbeck, E. and Friedrich, M. (2008) Evolution of insect eyes: tale of ancient heritage, deconstruction, reconstructions, remodeling, and recycling. *Evo Edu Outreach* **1**: 448–462.

Campbell, D. and Holt, C. (2001) Chemotropic responses of retinal growth cones mediated by rapid local protein synthesis. *Neuron* **32**: 1013–1026.

Cao, W., Epsien, C., Liu, H., Deloughery, C., Ge, N., Lin, J. *et al*. (2001) Comparing gene discovery from Affymetrix genechip microarrays and Clontech PCR-select cDNA subrtraction: a case study. *BMC Genomics* **5**: 26–35.

Clifford, K. (1980) Sterochemistry of the hydrolysis of trehalose by the enzyme trehalase prepared from the flesh fly *Sarcophaga barbata*. *Eur J Biochem* **106**:337–340.

Cline, H. and Haas, K. (2008) The regulation of dendritic arbor development and plasticity by glutamatergic synaptic input: a review of the synaptotrophic hypothesis. *J Physiol* **586**: 1509–1517.

Coimbra, A. (1966) Evaluation of the glycogenolytic effect of alpha-amylase using radioautography and electron microscopy. *J Histochem Cytochem* **14**: 898–906.

De Winter, F., Oudega, M., Lankhorst, A., Hamers, F., Blits, B.,

Ruitenberg, M. *et al*. (2002) Injury-induced class 3 semaphorin expression in the rat spinal cord. *Exp Neurol* **175**: 61–75.

Deitch, J. and Rubel, E. (1984) Afferent influences on brain stem auditory nuclei of the chicken: time course and specificity of dendritic atrophy following deafferentation. *J Comp Neurol* **10**: 66–79.

Derks, N., Muller, M., Gaxzner, B., Tilburg-Ouwens, D., Roubos, E. and Kozicz, L. (2008) Housekeeping genes revisited: different expressions depending on gender, brain area and stressor. *Neuroscience* **156**: 305–309.

DiAntonio, A. and Hicke, L. (2004) Ubiquitin-dependent regulation of the synapse. *Annu Rev Neurosci* **27**: 223–246.

Diatchenko, L., Lau, Y., Campbell, A., Chenchik, A., Moqadam, F., Huang, B. *et al*. (1996) Suppression subtractive hybridization: a method for generating differentially regulated or tissue-specific cDNA probes and libraries. *Proc Natl Acad Sci USA* **93**: 6025–6030.

Dmetrichuk, J., Carlone, R. and Spencer, G. (2006) Retinoic acid induces neurite outgrowth and growth cone turning in invertebrate neurons. *Dev Biol* **294**: 39–49.

Duester, G. (1994) Retinoids and the alcohol dehydrogenase gene family. *EXS* **71**: 279–290.

Furrer, M.-P., Kim, S., Wolf, B. and Chiba, A. (2003) Robo and frazzled/DCC mediate dendritic guidance at the CNS midline. *Nature Neurosci* **6**: 223–230.

Genikhovich, G., Kurn, U., Hemmrich, G. and Bosch, T. (2006) Discovery of genes expressed in *Hydra* embryogensis. *Dev Biol* **289**: 466–481.

Hegde, A. and DiAntonio, A. (2002) Ubiquitin and the synapse. *Nature Rev Neurosci* **3**: 854–861.

Hoy, R.R., Nolen, T.G. and Casaday, G.C. (1985) Dendritic sprouting and compensatory synaptogenesis in an identified interneuron following auditory deprivation in a cricket. *Proc Natl Acad Sci USA* **82**: 7772–7776.

Huber, F., Kleindienst, H.U., Weber, T. and Thorson, J. (1984) Auditory behavior of the cricket. III. Tracking of male calling song by surgically and developmentally one-eared females, and the curious role of the anterior tympanum. *J Comp Physiol [A]* **155**: 725–738.

Ing, B., Shteiman-Kotler, A., Castelli, M., Henry, P., Pak, Y., Stewart, B. *et al*. (2007) Regulation of commissureless by the ubiquitin ligase DNedd4 is required for neuromuscular synaptogenesis in *Drosophila melanogaster*. *Mol Cell Biol* **27**: 481–496.

Jahagirdar, A., Downer, R. and Viswantha, T. (1984) Influence of octopamine on trehalase activity in muscle and hemolymph of the American cockroach *Periplaneta americana*. *Biochim Biophys Acta* **801**: 177–183.

Jones, H., Ostrowski, M. and Scanlan, D. (2006) A suppression subtractive hybridization approach reveals niche-specific genes that may be involved in predator avoidance in marine *Synechococcus* isolates. *Appl Environ Microbiol* **72**: 2730–2737.

Kim, S. and Chiba, A. (2004) Dendritic guidance. *Trends Neurosci* **27**: 194–202.

Kwak S. and Matus A. (1988) Denervation induces long-lasting changes in the distribution of microtubule proteins in hippocampal neurons. *J Neurocytol* **17**: 189–195.

Lakes, R., Kalmring, K. and Engelhard, K.H. (1990) Changes in the auditory system of locusts (*Locusta migratoria* and *Schistocerca gregaria*) after deafferentation. *J Comp Physiol [A]* **166**: 553–563.

Lomax, M., Huang, L., Cho, Y., Gong. T.-W. and Altschuler, R. (2000) Differential display and gene arrays to examine auditory plasticity. *Hearing Res* **147**: 293–302.

Luthi, T.E. (1994) Molecules that become redistributed during regeneration of the leech central nervous system. *J Exp Biol* **186**: 43–54.

Maden, M. (2001) Role and distribution of retinoic acid during CNS development. *Int Rev Cytol* **209**: 1–77.

McAllister, A.K. (2000) Cellular and molecular mechanisms of dendrite growth. *Cereb Cortex* **10**: 963–973.

Miranda, J.D., White, L.A., Marcillo, A.E., Willson, C.A., Jagid, J. and Whittemore, S.R. (1999) Induction of Eph B3 after spinal cord injury. *Exp Neurol* **156**: 218–222.

Morgese, V., Elliott, E. and Muller, K. (1983) Microglial movement to sites of nerve lesion in the leech CNS. *Brain Res Prot* **272**: 166–170.

Mostafapour, S., Mae del Puerto, N. and Rubel, E. (2002) bcl-2 overexpression eliminates deprivation-induced cell death of brainstem auditory neurons. *J Neurosci* **22**: 4670–4674.

Murphey, R.K., Mendenhall, B., Palka, J. and Edwards, J.S. (1975) Deafferentation slows the growth of specific dendrites of identified giant interneurons. *J Comp Neurol* **159**: 407–418.

Myat, A., Henry, P., McCabe, V., Flintoft, L., Rotin, D. and Tear, G. (2002) *Drosophila* Nedd4, a ubiquitin ligase, is recruited by commissureless to control cell surface levels of the roundabout receptor. *Neuron* **35**: 447–459.

Niclou, S., Ehlert, E. and Verhaagen, J. (2006) Chemorepellent axon guidance molecules in spinal cord injury. *J Neurotrauma* **23**: 409–421.

Pallas, S.L. and Hoy, R.R. (1986) Regeneration of normal afferent input does not eliminate aberrant synaptic connections of an identified auditory interneuron in the cricket, *Teleogryllus oceanicus*. *J Comp Neurol* **248**: 348–359.

Parks, T. (1979) Afferent influences on the development of the brain stem auditory nuclei of the chicken: otocyst ablation. *J Comp Neurol* **183**: 665–678.

Pernas-Alonso, R., Morelli, F., di Porzio, U. and Perrone-Capano, C. (1999) Multiplex semi-quantitative reverse transcriptase-polymerase chain reaction of low abundance neuronal mRNAs. *Brain Res Prot* **4**: 395–406.

Pinter, M., Lent, D. and Strausfeld, N. (2006) Memory consolidation and gene expression in *Periplaneta americana*. *Learn Mem* **12**: 30–38.

Polleux, F., Morrow, T. and Ghosh, A. (2000) Semaphorin 3A is a chemoattractant for cortical apical dendrites. *Nature* **404**: 567–573.

Pyapali, G. and Turner, D. (1994) Denervation-induced dendritic alterations in CA1 pyramidal cells following kainic acid hippocampal lesions in rats. *Brain Res* **652**: 279–290.

Qin, M., Zeng, Z., Zheng, J., Shah, P., Schwartz, S., Adams, L. *et al.* (2003) Suppression subtractive hybridization identifies distinctive expression markers for coronary and internal mammary arteries. *Vacular Biol* **23**: 425–433.

Rawson, N. and LaMantia, A. (2006) Once and again: retinoic acid signaling in the developing and regenerating olfactory pathway. *J Neurobiol* **66**: 653–676.

Rozen, S. and Skaletsky, H. (2000) Primer3 on the WWW for general users and for biologist programmers. In *Bioinformatics Methods and Protocols: Methods in Molecular Biology* (Krawetz, S., Misener, S., Krawetz, S. and Misener, S.S., eds), pp. 365–386. Humana Press, Totowa, NJ.

Ruan, W. and Lai, M. (2007) Actin, a reliable marker of internal control? *Clinica Chimica Acta* **385**: 1–5.

Schafer, R., Dehn, D., Burbach, G. and Deller, T. (2008) Differential regulation of chondroitin sulfate proteoglycan mRNAs in the denervated rat fascia dentata after unilateral entorhinal cortex lesion. *Neurosci Lett* **439**: 61–65.

Schildberger, K., Wohlers, D.W., Schmitz, B., Kleindienst, H.U. and Huber, F. (1986) Morphological and physiological changes in central auditory neurons following unilateral foreleg amputation in larval crickets. *J Comp Physiol [A]* **158**: 291–300.

Schmid-Hempel, P. (2005) Evolutionary ecology of insect immune defenses. *Annu Rev Entomol* **50**: 529–551.

Schmitz, B. (1989) Neuroplasticity and phonotaxis in monaural adult female crickets (*Gryllus bimaculatus* Degeer). *J Comp Physiol [A]* **164**: 343–358.

Scott, E.K. and Luo, L. (2001) How do dendrites take their shape? *Nature Neurosci* **4**: 359–365.

Sherrard, R. and Bower, A. (1998) Role of afferents in the development and cell survival of the vertebrate nervous system. *Clin Exp Pharm Physiol* **25**: 487–495.

Son, T., Zou, Y., Jung, K., Yu, B., Ishigami, A., Maruyama, N. *et al.* (2006) SMP30 deficiency causes increased oxidative stress in brain. *Mech Ageing Dev* **127**: 451–457.

Sorensen, S. and Rubel, E. (2006) The level and integrity of synaptic input regulates dendritic structure. *J Neurosci* **26**: 1539–1550.

Steward, O. and Rubel. E. (1985) Afferent influences on brain stem auditory nuclei of the chicken: cessation of amino acid incorporation as an antecedent to age-dependent transneuronal degeneration. *J Comp Neurol* **15**: 385–395.

Sutton, M. and Schuman, E. (2005) Local translational control in dendrites and its role in long-term synaptic plasticity. *J Neurobiol* **64**: 116–131.

Twiss, J., Smith, D., Chang, B. and Shooter, E. (2000) Translational control of ribosomal protein L4 mRNA is required for rapid neurite regeneration. *Neurobiol Dis* **7**: 416–428.

Varshavsky, A. (1997) The N-end rule pathway of protein degradation. *Genes to Cells* **2**: 13–28.

Vaughn, J. (1989) Fine structure of syaptogenesis in the vertebrate central nervous system. *Synapse* **3**: 255–285.

Wang, W.-Z., Emes, R.D., Christoffers, K., Verrall, J. and Blackshaw, S.E. (2005) Hirudo medicinalis: a platform for investigating genes in neural repair. *Cell Mol Neurobiol* **25**: 427–440.

Wang, Y. and Rubel, E. (2008) Rapid regulation of microtubule-associated protein **2** in dendrites of nucleus laminaris of the chick following deprivation of afferent activity. *Neuroscience* **154**: 381–389.

Whitford, K., Marillat, V., Stein, E., Goodman, C., Tessier-Lavigne, M., Chedotal, A. *et al.* (2002) Regulation of cortical dendrite development by slit-robo interactions. *Neuron* **3**: 47–61.

Willmann, R. (2004) Phylogenetic relationships and evolution of insects. In *Assembling the Tree of Life* (Cracraft, J., Donoghue, M., Cracraft, J., Donoghue, M.s., eds), pp. 330–344. Oxford University Press, New York, NY.

Xu, X-Z., Wes, P., Chen, H., Li, H-S., Yu, M., Morgan, S. *et al.* (1998) Retinal targets for calmodulin include proteins implicated in synaptic transmission. *J Biol Chem* 47: 31297–31307.

Zhao, Y., Hegde, A. and Martin, K. (2003) The ubiquitin proteasome system functions as an inhibitory constraint on synaptic strengthening. *Curr Biol* **13**: 887–898.

